Contribution from the Department of Chemistry,
Michigan State University, East Lansing, Michigan 48824

Chemistry of Tris(2,4,6-trimethoxyphenyl)phosphine (TMPP) with Dirhodium Tetraacetate: Synthesis and Spectroscopic, Electrochemical, and Structural Characterization of a Binuclear Complex That Contains an Unusual Phenoxy-Phosphine Ligand

S. J. Chen and K. R. Dunbar*

Received September 14, 1990

Reaction of the ether-phosphine tris(2,4,6-trimethoxyphenyl)phosphine (TMPP) with $Rh_2(O_2CCH_3)_4(MeOH)_2$ in refluxing ethanol produces the demethylated phosphine compound $Rh_2(O_2CCH_3)_3$(TMPP-*O*)(MeOH)·EtOH in 60–65% yield (TMPP-*O* = oxygen metalated TMPP). The new complex has been fully characterized by ^1H NMR including COSY, $^{31}P\{^1H\}$ NMR and electronic spectroscopies as well as by electrochemistry and a single-crystal X-ray analysis. Crystals of **1** are triclinic, space group $P\bar{1}$, with unit cell parameters a = 13.730 (3) Å, b = 14.396 (5) Å, c = 11.921 (5) Å, α = 109.65 (2)°, β = 95.65 (2)°, γ = 64.32 (2)°, V = 1997 (1) Å^3, and Z = 2. The molecule consists of a dirhodium unit bridged by three acetate ligands and one demethylated TMPP ligand that forms two separate metallacycle rings with the rhodium atoms. In addition, there is one axial methanol ligand in the coordination sphere and an ethanol molecule in the lattice. The structure reveals that the tertiary phosphine adopts an unusual combination bridging/chelating bonding mode that involves a formal metallation of an *o*-methoxy group to give a phenoxy-phosphine ligand. The Rh–Rh distance is 2.4228 (3) Å, which is in the range found for a variety of tetrabridged Rh(II,II) complexes. Electrochemical measurements in solutions containing tetra-*n*-butylammonium hexafluorophosphate revealed a one-electron oxidation at $E_{1/2}$ = +0.71 V in THF and at +0.78 V vs Ag/AgCl in CH_3CN corresponding to the process $Rh_2^{4+} \rightarrow Rh_2^{5+}$. We have prepared the paramagnetic oxidation product by chemical methods and studied its behavior by electrochemistry, NMR and EPR spectroscopy.

Introduction

Phosphine ligands have played a pivotal role in the development of low-valent transition-metal chemistry, especially in the study of reactive, coordinatively unsaturated molecules.[1] In the case of triphenylphosphine, the lability of the ligand prompted Wilkinson and others to study its use in preparing Rh(I) and Rh(III) catalysts, and the successful use of PPh_3 in many homogeneously catalyzed reactions has since been widely supported.[2] Researchers have also shown that bulky tertiary phosphine ligands such as P(mesityl)$_3$,[3] P(*o*-tolyl)$_3$[4] or P(Cy)$_3$[5] can be used to design complexes with unusual geometries and properties, work that has prompted our recent interest in the chemistry of the bulky and basic phosphine ligand tris(2,4,6-trimethoxyphenyl)phosphine (TMPP).[6] Since both oxygen and phosphorus atoms are good

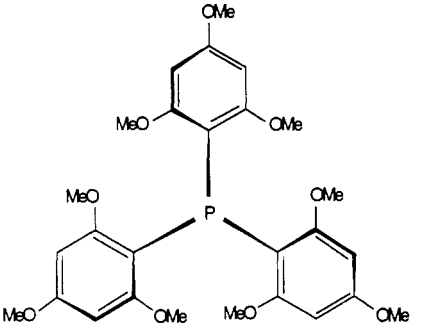

TMPP

donors, we predicted that the ligand could function as a unidentate *or* polydentate group depending upon the steric and electronic

(1) See for example: (a) Malatesta, L.; Cariello, C. *J. Chem. Soc.* **1958**, 2323. (b) Ugo, R.; Cariati, F.; LaMonica, G. *Inorg. Synth.* **1971**, *11*, 1707. (c) Ugo, R. *Coord. Chem. Rev.* **1968**, *3*, 105. (d) Alyea, E. C.; Meek, D. W. *Catalytic Aspects of Metal Phosphine Complexes*; Advances in Chemistry Series 196; American Chemical Society: Washington, DC, 1982. (e) Pignolet, L. H. *Homogeneous Catalysis With Metal Phosphine Complexes*; Plenum Press: New York, 1983.

(2) See for example: (a) Kosolapoff, G. F.; Maier, L. *Organic Phosphorus Compounds*; Wiley-Interscience: New York, 1972. (b) Cadogan, J. I. G. *Organophosphorus Reagents in Organic Synthesis*; Academic Press: London, 1979. (c) Gillard, R. D.; Osborn, J. A.; Stockwell, P. B.; Wilkinson, G. *Proc. Chem. Soc.* **1964**, 284. (d) Gillard, R. D.; Osborn, J. A.; Wilkinson, G. *J. Chem. Soc.* **1965**, 1951. (e) Osborn, J. A.; Wilkinson, G.; Young, J. F. *Chem. Commun.* **1965**, 17. (f) Young, J. F.; Osborn, J. A.; Jardine, F. H.; Wilkinson, G. *Chem. Commun.* **1965**, 131. (g) Baird, M. C.; Lawson, D. N.; Mague, J. T.; Osborn, J. A.; Wilkinson, G. *Chem. Commun.* **1966**, 129. (h) Baird, M. C.; Mague, J. T.; Osborn, J. A.; Wilkinson, G. *J. Chem. Soc. A* **1967**, 1347. (i) Jardine, F. H.; Osborn, J. A.; Wilkinson, G. *J. Chem. Soc. A* **1967**, 1574. (j) Roundhill, D. M.; Lawson, D. N.; Wilkinson, G. *J. Chem. Soc. A* **1968**, 845. (k) Singer, H.; Wilkinson, G. *J. Chem. Soc. A* **1968**, 849. (l) Montelatici, S.; van der Ent, A.; Osborn, J. A.; Wilkinson, G. *J. Chem. Soc. A* **1968**, 1054. (m) O'Connor, C.; Yagupsky, G.; Evans, D.; Wilkinson, G. *Chem. Commun.* **1968**, 420. (n) Evans, D.; Yagupsky, G.; Wilkinson, G. *J. Chem. Soc. A* **1968**, 2660. (o) Evans, D.; Osborn, J. A.; Wilkinson, G. *J. Chem. Soc. A* **1968**, 3133. (p) Wilkinson, G. *Bull. Soc. Chim. Fr.* **1968**, *12*, 5055.

(3) (a) Halpern, E. J.; Mislow, K. *J. Am. Chem. Soc.* **1967**, *89*, 5224. (b) Blount, J. F.; Maryanoff, C. A.; Mislow, K. *Tetrahedron Lett.* **1975**, *11*, 913. (c) Alyea, E. C.; Dias, S. A.; Ferguson, G.; Parvez, M. *Inorg. Chim. Acta* **1979**, *37*, 45. (d) Dias, S. A.; Alyea, E. C. *Trans. Met. Chem. (Weinheim, Ger.)* **1979**, *4*, 205. (e) Alyea, E. C.; Ferguson, G.; Somogyvari, A. *Inorg. Chem.* **1982**, *21*, 1369. (f) Alyea, E. C.; Malito, J. *J. Organomet. Chem.* **1988**, *340*, 119.

(4) (a) Bowden, J. A.; Colton, R. *Aust. J. Chem.* **1971**, *24*, 2471. (b) Bennett, M. A.; Bramley, R.; Longstaff, P. A. *J. Chem. Soc., Chem. Commun.* **1966**, 806.

(5) (a) Ferguson, G.; Roberts, P. J.; Alyea, E. C.; Khan, M. *Inorg. Chem.* **1978**, *17*, 2965. (b) Kubas, G. J.; Ryan, R. R.; Swanson, B. I.; Vergamini, P. J.; Wasserman, H. J. *J. Am. Chem. Soc.* **1984**, *106*, 451. (c) Kubas, G. J.; Unkefer, C. J.; Swanson, B. I.; Fukushima, E. *J. Am. Chem. Soc.* **1986**, *108*, 7000. (d) Darensbourg, D. J.; Darensbourg, M. Y.; Gob, L. Y.; Ludvig, M.; Wiegreffe, P. *J. Am. Chem. Soc.* **1987**, *109*, 7539. (e) Clark, H. C.; Hampden-Smith, M. J. *Coord. Chem. Rev.* **1987**, *79*, 229 and references therein. (f) Gonzalez, A. A.; Mukerjee, S. L.; Chou, S.-J.; Kai, Z.; Hoff, C. D. *J. Am. Chem. Soc.* **1988**, *110*, 4419. (g) Kubas, G. J. *Comments Inorg. Chem.* **1988**, *7*, 17. (h) Esteruelas, M. A.; Sola, E.; Oro, L. A.; Meyer, U.; Werner, H. *Angew. Chem., Int. Ed. Engl.* **1988**, *27*, 1563. (i) Kubas, G. J. *Acc. Chem. Res.* **1988**, *21*, 120. (j) Arliguie, T.; Chauchet, B.; Jalon, F.; Lahoz, F. *J. Chem. Soc., Chem. Commun.* **1988**, 998. (k) Arliguie, T.; Chauchet, B.; Morris, R. H.; Sella, A. *Inorg. Chem.* **1988**, *27*, 598. (l) Crocker, L. S.; Heinekey, D. M.; Schulte, G. K. *J. Am. Chem. Soc.* **1988**, *110*, 405.

(6) (a) Wada, H.; Higashizaki, S. *J. Chem. Soc., Chem. Commun.* **1984**, 482. (b) Wada, M.; Higashizaki, S.; Tsuboi, A. *J. Chem. Res., Synop.* **1985**, 38. (c) Wada, M. *Yuki Gosei Kagaku Kyokaishi* **1986**, 957. (d) Wada, M.; Tsuboi, A. *J. Chem. Soc., Perkin Trans. 1* **1987**, 151. (e) Bowmaker, G. A.; Cotton, J. D.; Healy, P. C.; Kildea, J. D.; Silong, S. B.; Skelton, B. W.; White, A. H. *Inorg. Chem.* **1989**, *28*, 1462. (f) Dunbar, K. R.; Haefner, S. C.; Pence, L. E. *J. Am. Chem. Soc.* **1989**, *111*, 5504. (g) Dunbar, K. R.; Haefner, S. C.; Burzynski, D. J. *Organometallics* **1990**, *9*, 1347. (h) Chen, S. J.; Dunbar, K. R. *Inorg. Chem.* **1990**, *29*, 588; see also references therein. (i) Dunbar, K. R.; Haefner, S. C.; Quillevéré, A. *Polyhedron* **1990**, *9*, 1695. (j) Dunbar, K. R.; Haefner, S. C. *J. Chem. Soc., Chem. Commun.*, in press.

0020-1669/91/1330-2018$02.50/0

preferences of the metal center. Indeed, we have structurally characterized a number of complexes which exhibit the monodentate coordination mode,[6j] chelating bidentate mode,[6j] and chelating tridentate mode.[6f,g]

(1) Chelating modes

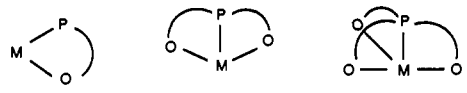

(2) Bridging modes

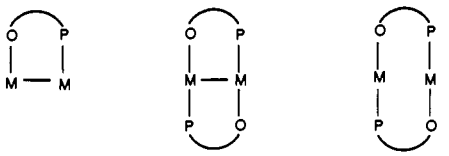

(3) Bridging and chelating mode

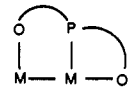

In this paper, we report a new type of coordination for TMPP in which the ligand is both bridging and chelating two metal centers. It is evident from these and earlier studies that TMPP is a good donor ligand for both early- and late-transition-metal centers and that it exhibits a considerable amount of flexibility in its coordination geometries. Additionally, the ligand can be considered a good nucleating group for preventing the fragmentation of multimetallic complexes, such as dimer and cluster systems.

In our design of experiments to synthesize binuclear complexes of TMPP, we chose to focus on the three basic systems depicted as **A**–**C**. In the first group are starting materials with the lantern

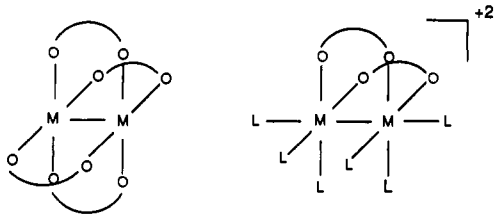

(L = MeCN)

A **B**

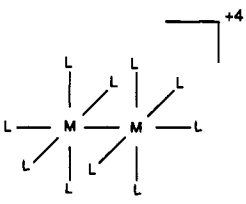

(L = MeCN)

C

structure, the most common examples being tetrakis(carboxylato) complexes (**A**). The second type of starting material, **B**, is one possessing two cis carboxylate ligands and labile neutral donors. The third system under investigation is the fully solvated binuclear cation, **C**, with all coordination sites occupied by labile acetonitrile ligands. We are interested in comparing the TMPP chemistry of these three classes of compounds, particularly with respect to their ease of substitution and metal–metal bond scission. In this paper we limit our discussion to the chemistry of type **A** complexes, specifically reactions of dirhodium tetraacetate with tris(2,4,6-trimethoxyphenyl)phosphine.

Herein, we report the synthesis of two related dirhodium compounds with a bridging and chelating form of the TMPP ligand, the existence of which lends support to our predictions regarding the flexibility and diverse reactivity of this interesting ligand. A preliminary communication of part of this work has appeared in the literature.[6h]

Experimental Section

General Procedures. The starting materials $Rh_2(O_2CCH_3)_4(MeOH)_2$[7] and TMPP[8] were prepared according to published methods. Solvents were dried over appropriate drying agents and freshly distilled before use. Reactions were carried out under an argon atmosphere by using standard Schlenk-line techniques.

A. Preparation of $Rh_2(O_2CCH_3)_3$(TMPP-*O*)(MeOH) (1). A suspension of $Rh_2(O_2CCH_3)_4(MeOH)_2$ (0.10 g, 0.2 mmol) and TMPP (0.21 g, 0.4 mmol) in ethanol (20 mL) was refluxed for 6 h to give a clear green solution. The solvent was removed by vacuum distillation, and the resulting residue was extracted with 15 mL of methanol/diethyl ether (1:1 v/v). The green extract solution was filtered through a medium-porosity frit, concentrated to ca. 5 mL, and layered with diethyl ether (10 mL). A crop of green crystals was obtained after slow evaporation of the solution in air for several days; yield 0.118 g (64%). Crystalline samples that are subjected to a static vacuum for 24 h lose interstitial ethanol of crystallization and the labile axial methanol ligand, as evidenced by ^1H NMR spectroscopy and fast atom bombardment mass spectrometry (highest mass peak is m/z = 900.1 for $Rh_2(O_2CCH_3)_3$(TMPP-*O*)). Anal. Calcd for $C_{32}H_{39}O_{15}P_1Rh_2$: C, 42.51; H, 4.65. Found: C, 42.68; H, 4.37.

B. Reaction of 1 with $NOPF_6$. A solution of $NOPF_6$, (0.020 g, 0.11 mmol) in CH_3CN (5 mL) was slowly added to $Rh_2(O_2CCH_3)_3$(TMPP-*O*)(MeOH) (0.10 g, 0.11 mmol) in CH_3CN (10 mL). The green solution turned brown immediately, and after the mixture was stirred for 15 min, the solvent was removed by vacuum distillation. The dark orange-brown residue was extracted with 10 mL of CH_2Cl_2 after which diethyl ether (10 mL) was added to induce precipitation. A brown microcrystalline solid was collected on a medium-porosity frit under argon and dried under reduced pressure. The product was recrystallized by slow diffusion of diethyl ether into a CH_2Cl_2 solution of the compound.

Physical Measurements. ^1H NMR spectra were obtained on a Bruker 250-MHz or a Varian VXR 300-MHz spectrometer. ^{31}P NMR spectra were recorded on a Varian VXR 300-MHz spectrometer with an internal deuterium lock and 85% H_3PO_4 as an external standard. Infrared spectra were recorded on a Perkin-Elmer 599 or a Nicolet 740 FT-IR spectrophotometer. Electrochemical measurements were carried out by using an EG&G Princeton Applied Research Model 362 scanning potentiostat in conjunction with a BAS Model RXY recorder. Cyclic voltammetry was performed at 22 ± 2 °C in CH_3CN or THF containing 0.2 M tetra-*n*-butylammonium hexafluorophosphate (TBAH) as the supporting electrolyte. The working electrode was a BAS Pt disk electrode. $E_{1/2}$ values, determined as $(E_{p,a} + E_{p,c})/2$, were referenced to the Ag/AgCl electrode and are uncorrected for junction potentials. The ferrocene couple occurs at + 0.52 V vs Ag/AgCl under the same experimental conditions. Fast-atom-bombardment (FAB) mass spectrometry studies were performed on a JEOL HX 110 double-focusing mass spectrometer housed in the National Institutes of Health/Michigan State University Mass Spectrometry Facility; the sample was dissolved in a 3-nitrobenzyl alcohol matrix.

X-ray Structural Study of $Rh_2(O_2CCH_3)_3$(TMPP-*O*)(MeOH) (1). Data Collection and Reduction. The structure of **1** was determined by general procedures that have been fully described elsewhere.[9] A green crystal of dimensions 0.78 × 0.52 × 0.20 mm^3 was covered with epoxy cement and mounted at the end of a glass fiber. Geometric and intensity

(7) Rempel, G. A.; Legzdins, P.; Smith, H.; Wilkinson, G. *Inorg. Synth.* **1972**, *13*, 90.
(8) The communication listed in ref 6a gives very few experimental details; thus, we have developed our own high-yield method. Dunbar, K. R.; Haefner, S. C. Unpublished results.
(9) (a) Bino, A.; Cotton, F. A.; Fanwick, P. E. *Inorg. Chem.* **1979**, *18*, 3558. (b) Cotton, F. A.; Frenz, B. A.; Deganello, G.; Shaver, A. *J. Organomet. Chem.* **1973**, *50*, 227.

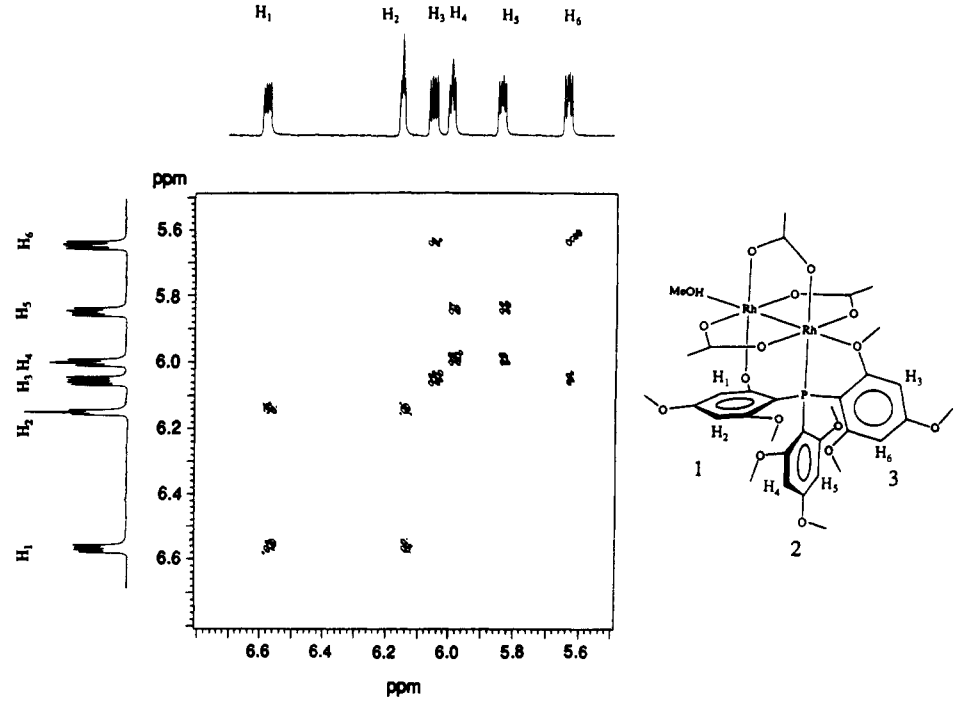

Figure 1. DQCOSY spectrum of **1** revealing the coupling of the ring protons.

data were obtained on a Nicolet P3/F diffractometer equipped with a graphite-monochromated Mo Kα radiation source. A rotation photograph was used to locate 15 reflections from which a preliminary cell was indexed. The reduced cell dimensions indicated that the crystal was triclinic, which was confirmed by axial photography. An accurate cell for data collection was calculated from 20 reflections with 2θ values between 20° and 30°. A hemisphere of data was measured in the range $+h,+k,+l$ by an ω–2θ scan motion to give 7053 data points with $4 \leq 2\theta \leq 50°$.

Data reduction was carried out by standard methods.[10] The structure factors were obtained after correction for Lorentz and polarization effects. During data collection, three check reflections were measured every 100 reflections; no loss in intensity was observed, and thus a correction was not applied.

Structure Solution and Refinement. Programs from the Enraf-Nonius Structure Determination Package were used to solve and refine the structure. The positions of the Rh atoms were calculated from a Patterson Fourier map. A sequence of successive difference Fourier maps and least-squares cycles led to full development of the coordination sphere, excluding hydrogen atoms. The final full-matrix refinement involved 451 parameters and 6209 observations with $F_o^2 \geq 3\sigma(F_o)^2$ for a data-to-parameter ratio of 11.3. During the refinement, it became apparent that a disordered ethanol molecule was present as an interstitial solvent of crystallization. Several attempts to model this portion of the structure failed to produce chemically sensible results; thus, the three highest areas of electron density, which in fact constitute a reasonable bonding pattern for ethanol, were assigned full occupancy and fixed for the remainder of the refinement process. The highest peak in the final difference Fourier map is 1.6 e/Å^3 in the vicinity of the disordered ethanol unit C(34)–C(35)–O(17). After isotropic convergence had been achieved, an absorption correction based on the program DIFABS was applied to the data.[10b] The refinement converged with residuals of R = 0.0504 and R_w = 0.0858 with a quality of fit equal to 2.93. The largest shift/esd in the final cycle was 0.96.

Crystal parameters and basic information pertaining to data collection and structure refinements are summarized in Table I. Positional parameters and equivalent isotropic displacement parameters are listed in Table II. Complete tables of bond distances and angles, anisotropic thermal parameters, and structure factors are available as supplementary material.

Results

Synthesis. Reactions of $Rh_2(O_2CCH_3)_4(MeOH)_2$ with 2 equiv of the ether–phosphine ligand tris(2,4,6-trimethoxyphenyl)-

Table I. Crystal Data for $Rh_2(O_2CCH_3)_3[\{C_6H_2(OMe)_3\}_2P\{C_6H_2(OMe)_2O\}](MeOH)\cdot EtOH$

formula	$Rh_2P_1O_{17}C_{35}H_{49}$	Z	2
fw	978.547	d_{calc}, g/cm^3	1.633
space group	$P\bar{1}$	μ(Mo Kα), cm^{-1}	9.251
a, Å	13.730 (3)	radiation	Mo Kα (λ_α =
b, Å	14.396 (5)	(monochromated	0.71073 Å);
c, Å	11.921 (5)	in incident	graphite
α, deg	109.65 (2)	beam)	monochromated
β, deg	95.65 (2)	temp, °C	22 ± 2
γ, deg	64.32 (2)	R^a	0.0504
V, Å^3	1997 (1)	R_w^b	0.0858

$^a R = \sum||F_o| - |F_c||/\sum|F_o|$. $^b R_w = [\sum w|F_o| - |F_c|)^2/\sum w|F_o|^2]^{1/2}$; $w = 1/\sigma^2(|F_o|)$.

Scheme I

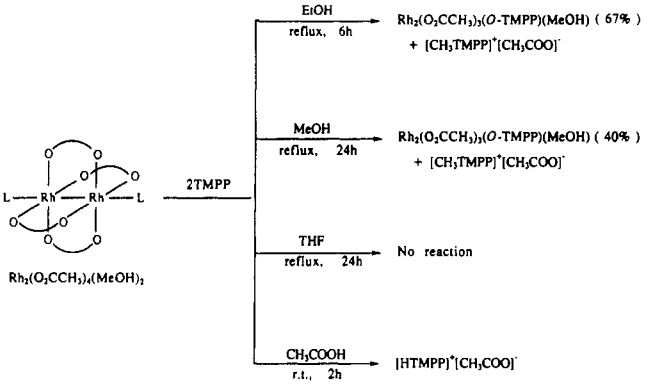

phosphine (TMPP) in refluxing alcohols produce the demethylation compound $Rh_2(O_2CCH_3)_3$(TMPP-*O*)(MeOH). One equivalent of phosphine is methylated to form $[H_3C{-}PR_3]^+$ as evidenced by ^{1}H NMR spectroscopic studies of residues retrieved from the filtrate. The reaction has been successfully performed in both methanol and ethanol, with the latter solvent producing a higher yield of **1** (67% versus 40%) for a shorter reflux time (6 h versus 24 h). The identical experiment in THF results in no observed reaction for reflux times up to several days; it appears that the reaction is facilitated by protic solvents. Attempts to obtain Rh_2TMPP complexes in acetic acid in the manner previously described by Cotton et al. proved to be unsuccessful. The highly basic TMPP (pK_b = 3) is easily protonated to the phos-

(10) (a) Crystallographic computing was done on a VAXSTATION-2000 with programs from the Enraf-Nonius SDP package. (b) Walker, N.; Stuart, D. *Acta Crystallogr., Sect. A, Found. Crystallogr.* **1983**, *A39*, 158.

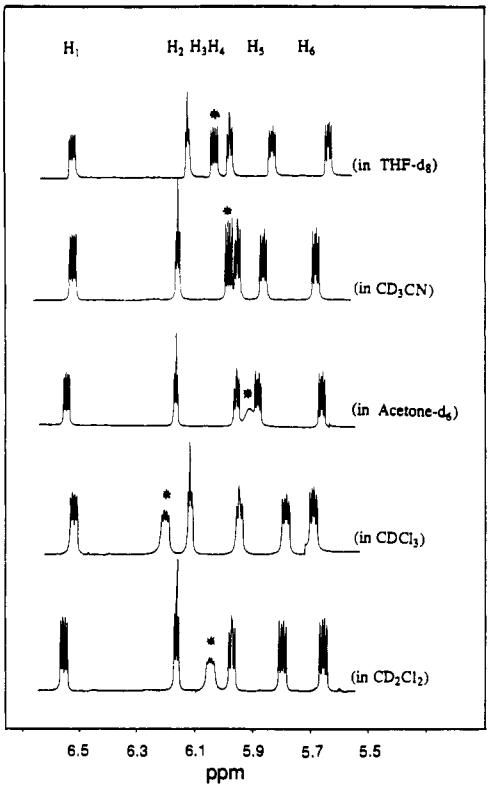

Figure 2. 300-MHz ^1H NMR spectra of **1** in various deuteriated solvents indicating the solvent dependence of H_3.

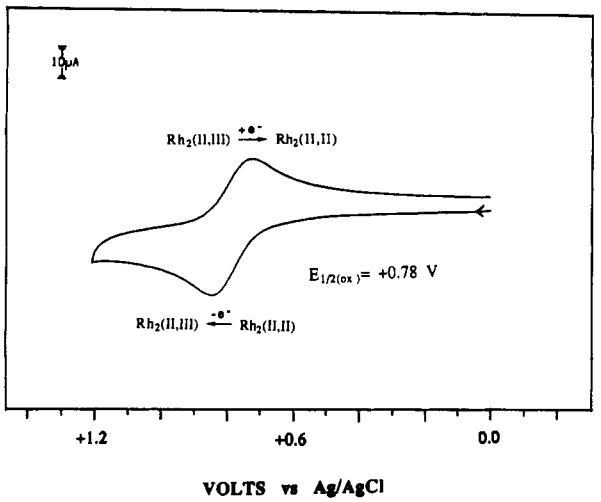

Figure 3. Cyclic voltammogram of **1** in 0.2 M tetra-*n*-butylammonium hexafluorophosphate–CH_3CN solution at 200 mV/s. The working electrode is a Pt disk and the reference electrode is Ag/AgCl.

phonium salt by CH_3COOH. A summary of reactions in this study is shown in Scheme I.

The characterization of $Rh_2(O_2CCH_3)_3$(TMPP-*O*)(MeOH) (**1**) and the one-electron oxidation product **2** was carried out by various spectroscopic techniques (Figures 1–5) and will be discussed in the following sections. In addition, the X-ray structure of **1**, the results of which are summarized in Tables I–III and Figure 6, will be described in full.

Discussion

NMR Spectroscopy. The room-temperature 300-MHz ^1H NMR spectrum of **1** in CD_3CN revealed that the TMPP ligand is ligated in a completely unsymmetrical fashion about the two metal centers. Four meta protons are well-resolved quartets and resonate at δ = 6.52, 5.96, 5.84, and 5.65 ppm; two ring protons appear as virtual triplets at δ = 6.15 and 5.93 ppm. After ^{31}P decoupling, all six meta protons are simplified into doublets. Eight

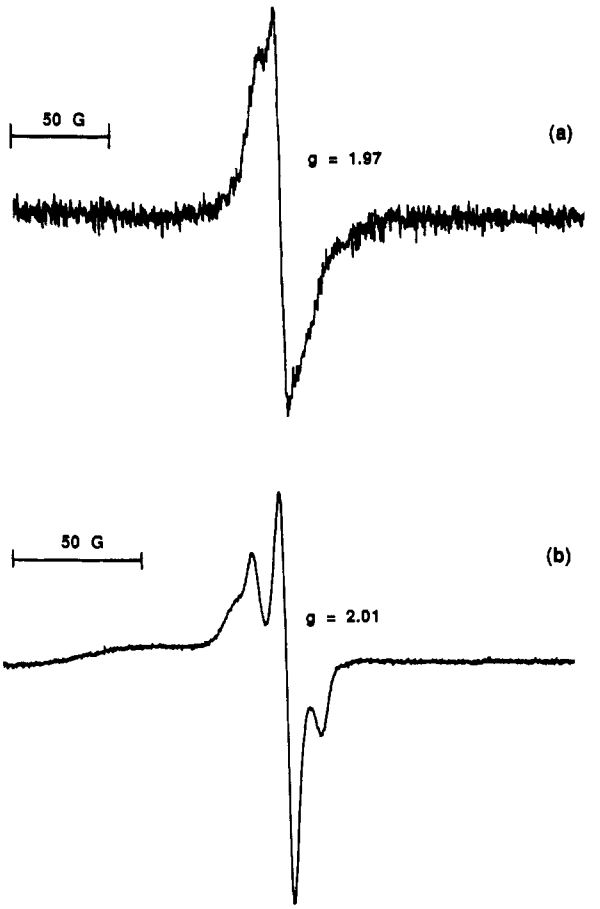

Figure 4. EPR spectrum of **1** (a) in the solid state at 130 K and (b) in frozen CD_3CN at 116 K.

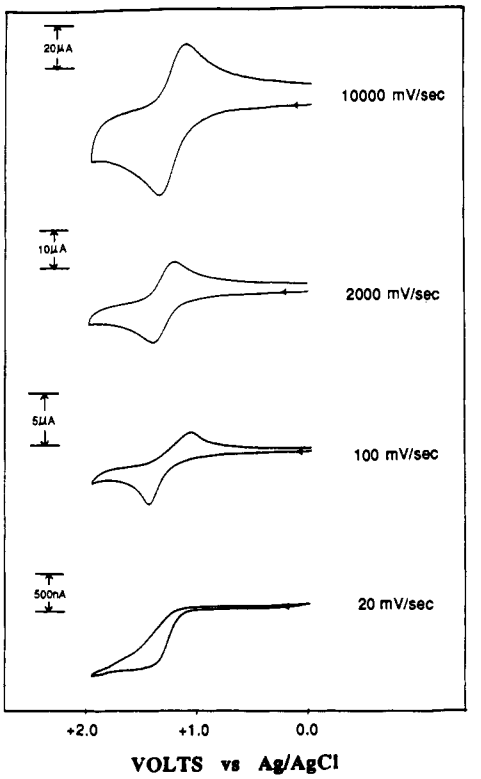

Figure 5. Variable-scan-speed cyclic voltammograms of **1** in CH_3CN emphasizing the irreversibility of the $Rh^{II}_2 \rightleftharpoons Rh^{II}Rh^{III}$ process.

methoxy group resonances were observed, with the most deshielded signal at δ = +2.57 ppm being assigned to the ring that participates in an axial interaction with the metal center. The absence of a

Table II. Atomic Positional Parameters and Equivalent Isotropic Displacement Parameters (Å^2) and Their Estimated Standard Deviations for $Rh_2(O_2CCH_3)_3[\{C_6H_2(OMe)_3\}_2P\{C_6H_2(OMe)_2O\}]MeOH\cdot EtOH$

atom	x	y	z	B^a
Rh(1)	0.97704 (3)	0.35229 (3)	0.23068 (3)	1.616 (8)
Rh(2)	1.05222 (3)	0.16371 (3)	0.10063 (3)	1.633 (8)
P(1)	0.81147 (9)	0.39684 (9)	0.1656 (1)	1.56 (2)
O(1)	1.0160 (3)	0.1217 (3)	0.2341 (3)	2.39 (8)
O(2)	0.9526 (3)	0.2964 (3)	0.3578 (3)	2.36 (8)
O(3)	1.1992 (3)	0.1453 (3)	0.1673 (3)	2.59 (9)
O(4)	1.1367 (3)	0.3189 (3)	0.2908 (3)	2.62 (9)
O(5)	1.0850 (3)	0.2156 (2)	−0.0239 (3)	2.09 (8)
O(6)	1.0172 (3)	0.3908 (2)	0.0974 (3)	2.10 (7)
O(7)	0.9073 (3)	0.1720 (2)	0.0311 (3)	2.13 (8)
O(8)	0.7923 (3)	0.1996 (3)	−0.3559 (3)	3.7 (1)
O(9)	0.7551 (3)	0.5140 (3)	−0.0299 (3)	2.60 (8)
O(10)	0.8996 (3)	0.5422 (3)	0.3292 (3)	2.37 (8)
O(11)	0.5873 (4)	0.8837 (3)	0.3734 (4)	4.2 (1)
O(12)	0.5893 (3)	0.5445 (3)	0.1251 (3)	2.72 (9)
O(13)	0.6669 (3)	0.2732 (3)	0.0387 (3)	2.37 (8)
O(14)	0.5279 (3)	0.2763 (3)	0.3873 (3)	3.81 (9)
O(15)	0.7465 (3)	0.4691 (3)	0.4123 (3)	2.25 (8)
O(16)	1.1367 (3)	−0.0100 (3)	−0.0216 (3)	2.46 (8)
C(1)	0.9731 (4)	0.1956 (4)	0.3316 (4)	2.4 (1)
C(2)	0.9446 (6)	0.1651 (5)	0.4282 (6)	4.0 (2)
C(3)	1.2114 (4)	0.2246 (4)	0.2467 (5)	2.5 (1)
C(4)	1.3242 (4)	0.2016 (5)	0.2902 (7)	4.3 (2)
C(5)	1.0588 (4)	0.3160 (4)	−0.0009 (5)	2.2 (1)
C(6)	1.0794 (5)	0.3496 (4)	−0.1012 (5)	3.0 (1)
C(7)	0.8189 (3)	0.3459 (3)	0.0054 (4)	1.6 (1)
C(8)	0.8645 (4)	0.2302 (4)	−0.0437 (4)	1.8 (1)
C(9)	0.8584 (4)	0.1762 (4)	−0.1651 (4)	2.2 (1)
C(10)	0.8120 (4)	0.2400 (4)	−0.2372 (4)	2.4 (1)
C(11)	0.7793 (4)	0.3520 (4)	−0.1969 (4)	2.2 (1)
C(12)	0.7836 (4)	0.4054 (4)	−0.0764 (4)	2.0 (1)
C(13)	0.8029 (7)	0.0907 (6)	−0.3968 (6)	5.6 (2)
C(14)	0.7219 (5)	0.5767 (4)	−0.1098 (5)	3.8 (1)
C(15)	0.7455 (4)	0.5449 (4)	0.2215 (4)	1.8 (1)
C(16)	0.7967 (4)	0.6035 (4)	0.3006 (4)	1.9 (1)
C(17)	0.7479 (4)	0.7165 (4)	0.3537 (5)	2.5 (1)
C(18)	0.6410 (4)	0.7717 (4)	0.3239 (5)	2.8 (1)
C(19)	0.5863 (4)	0.7171 (4)	0.2466 (5)	2.6 (1)
C(20)	0.6384 (4)	0.6050 (4)	0.1979 (4)	2.0 (1)
C(21)	0.9575 (4)	0.5982 (4)	0.4112 (6)	3.6 (1)
C(22)	0.6426 (8)	0.9460 (8)	0.4359 (9)	4.9 (2)*
C(22B)	0.490 (2)	0.939 (2)	0.350 (3)	4.8 (6)*
C(23)	0.4774 (4)	0.5774 (5)	0.1506 (5)	3.2 (1)
C(24)	0.7175 (4)	0.3623 (4)	0.2261 (4)	1.8 (1)
C(25)	0.6604 (4)	0.3032 (4)	0.1605 (4)	2.1 (1)
C(26)	0.5961 (4)	0.2759 (4)	0.2170 (5)	2.5 (1)
C(27)	0.5885 (4)	0.3106 (4)	0.3404 (5)	2.7 (1)
C(28)	0.6398 (4)	0.3735 (4)	0.4100 (5)	2.5 (1)
C(29)	0.7009 (4)	0.3997 (4)	0.3493 (4)	2.0 (1)
C(30)	0.6285 (4)	0.1932 (4)	−0.0299 (5)	2.9 (1)*
C(31)	0.5200 (5)	0.3026 (5)	0.5141 (6)	3.7 (1)*
C(32)	0.7495 (4)	0.4954 (4)	0.5390 (5)	2.8 (1)*
C(33)	1.1564 (5)	−0.0244 (4)	−0.1441 (5)	3.2 (1)*
C(34)[b]	0.625	0.996	0.028	32 (2)
C(35)[b]	0.625	0.916	0.082	13.1 (5)
O(17)[b]	0.563	0.875	0.027	28.5 (8)

[a] Starred values denote atoms that were refined isotropically. Values for anisotropically refined atoms are given in the form of the equivalent isotropic displacement parameter defined as $^4/_3[a^2\beta_{11} + b^2\beta_{22} + c^2\beta_{33} + ab(\cos\gamma)\beta_{12} + ac(\cos\beta)\beta_{13} + bc(\cos\alpha)\beta_{23}]$. [b] Lattice ethanol which was placed in fixed positions.

ninth methoxy group suggested that demethylation had occurred, which was subsequently confirmed by a solid-state structural determination (vide infra). The $^{31}P\{^1H\}$ spectrum in CD_3CN exhibits a doublet at $\delta = -9.8$ ppm with $J(^{103}Rh-^{31}P) = 159$ Hz.

The DQCOSY spectrum of **1** (Figure 1) clearly shows the J coupling between H_1 and H_2, H_3 and H_6, and H_4 and H_5 via their mutual cross-peaks. Due to the strong bonding between ring 1 and Rh(2) via a phenoxide interaction, we assign the most deshielded protons H_1 and H_2 to this ring. The two meta protons in the free phenyl ring have similar environments thus we assign

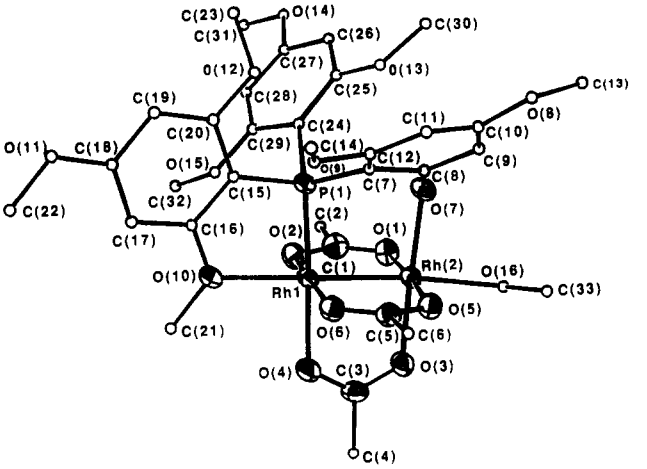

Figure 6. ORTEP representation of **1** with 50% probability ellipsoids. Phenyl group atoms are shown as small circles for clarity.

Table III. Selected Bond Distances (Å) and Bond Angles (deg) for $Rh_2(O_2CCH_3)_3[\{C_6H_2(OMe)_3\}_2P\{C_6H_2(OMe)_2O\}]MeOH\cdot EtOH$

Bond Distances			
Rh(1)–Rh(2)	2.4228 (3)	P(1)–C(24)	1.847 (3)
Rh(1)–P(1)	2.2135 (8)	O(1)–C(1)	1.257 (4)
Rh(1)–O(2)	2.050 (2)	O(2)–C(1)	1.280 (4)
Rh(1)–O(4)	2.134 (2)	O(3)–C(3)	1.277 (4)
Rh(1)–O(6)	2.038 (2)	O(4)–C(3)	1.258 (4)
Rh(1)–O(10)	2.351 (2)	O(5)–C(5)	1.262 (4)
Rh(2)–O(1)	2.049 (2)	O(6)–C(5)	1.265 (4)
Rh(2)–O(3)	2.034 (2)	O(7)–C(8)	1.345 (4)
Rh(2)–O(5)	2.030 (2)	O(10)–C(16)	1.384 (4)
Rh(2)–O(7)	2.048 (2)	O(16)–C(33)	1.437 (4)
Rh(2)–O(16)	2.251 (2)	C(7)–C(8)	1.418 (4)
P(1)–C(7)	1.793 (3)	C(15)–C(16)	1.394 (4)
P(1)–C(15)	1.813 (3)		

Bond Angles			
Rh(2)–Rh(1)–P(1)	95.92 (2)	Rh(1)–P(1)–C(15)	105.0 (1)
Rh(2)–Rh(1)–O(2)	86.69 (7)	Rh(1)–P(1)–C(7)	109.6 (1)
Rh(2)–Rh(1)–O(4)	86.51 (6)	Rh(2)–O(7)–C(8)	118.2 (2)
Rh(2)–Rh(1)–O(6)	87.67 (6)	Rh(1)–O(10)–C(16)	117.8 (2)
Rh(2)–Rh(1)–O(10)	171.05 (6)	Rh(2)–O(16)–C(33)	116.2 (2)
P(1)–Rh(1)–O(10)	80.06 (6)	P(1)–C(7)–C(8)	114.0 (2)
Rh(1)–Rh(2)–O(1)	88.65 (7)	O(7)–C(8)–C(7)	118.1 (3)
Rh(1)–Rh(2)–O(7)	94.57 (6)	P(1)–C(15)–C(16)	120.5 (2)
O(7)–Rh(2)–O(16)	90.06 (9)	O(10)–C(16)–C(15)	116.1 (3)

protons H_4 and H_5 to ring 2. Finally, H_3 and H_6 are in the same ring based on correlated cross-peaks, and a further study reveals that the chemical shift of H_3 is very solvent dependent. The meta proton region of **1** between 5.0 and 6.5 ppm in five different deuteriated solvents are shown in Figure 2. The quartet denoted by an asterisk symbol (H_3 in CD_3CN) shifts downfield in THF-d_8, $CDCl_3$, and CD_2Cl_2. In acetone-d_6, the resonance broadens and shifts upfield. These observations are consistent with axial ether group exchange with the solvent. The ring proton in close proximity to the axial methoxy ligand (H_3) would be expected to be affected most dramatically by the chemical environment of this position.

The Bruker simulation program PANIC was utilized to obtain further coupling constant information: $J_{H_1H_2} = 1.94$ Hz, $J_{H_1P} = 4.20$ Hz, $J_{H_2P} = 2.15$ Hz, $J_{H_3H_6} = 2.37$ Hz, $J_{H_3P} = 4.60$ Hz, $J_{H_6P} = 4.00$ Hz, $J_{H_4H_5} = 2.15$ Hz, $J_{H_4P} = 2.70$ Hz, and $J_{H_5P} = 3.91$ Hz. The smaller coupling constants J_{H_2P} and J_{H_4P} are consistent with the observation that both triplets of H_2 and H_4 are due to a second-order effect.

Electrochemistry and Chemical Oxidation of 1. The cyclic voltammogram of $Rh_2(O_2CCH_3)_3(TMPP)(MeOH)$ exhibits a one-electron quasi-reversible oxidation at +0.78 V in CH_3CN vs. Ag/AgCl at 200 mV/s (Figure 3). Oxidative bulk electrolysis of complex **1** in CH_3CN at 1.0 V is accompanied by a color change from green to orange-brown. We were unsuccessful in isolating the oxidation product by this method, due mainly to the difficulty

in separating it from the supporting electrolyte. However, chemical oxidation of $Rh_2(O_2CCH_3)_3$(TMPP-*O*)(MeOH) by reaction with 1 equiv of $NOPF_6$ yields a red-brown solid, **2**, which was investigated by several spectroscopic methods. The broad and featureless ^1H NMR spectrum clearly indicated that the compound is paramagnetic, thus supporting the formulation as an Rh_2^{5+} species. The IR spectrum of **2** exhibits an absorption at 845 cm^{-1}, which corresponds to the P–F stretch of the PF_6^- counterion; there is no evidence for a coordinated NO group. Additional data to support the formulation of the product as one containing a paramagnetic rhodium cation is the ^{31}P NMR spectrum, which shows a single (heptet) resonance at ca −100 ppm due to the PF_6^- anion but no resonance for the phosphine ligand. A solid-state EPR spectrum of **2** at 130 K exhibited a featureless signal at g = 1.97, whereas a frozen CD_3CN solution at 116 K gave a three line signal centered at g = 2.01 (Figure 4). On the basis of the aforementioned data, we formulate the oxidation product as a formal Rh_2^{5+} species. Since the cyclic voltammogram of the parent Rh_2^{4+} compound showed a nearly reversible oxidation couple, we expected the chemically oxidized product to be closely related structurally, thus exhibiting a reduction couple at a potential close to $E_{1/2}$ = +0.78 in CH_3CN. Surprisingly, we did not observe any accessible electrochemical processes in the cyclic voltammogram of **2**. This led us to further investigate the electrochemistry of **1** at various scan speeds (Figure 5). A reversible couple was observed at high scan rates (10 000 down to 100 mV/s), but at slower scan speeds (100 to 20 mV/s), the oxidation wave clearly becomes irreversible. These results suggest that the formation of **2** by the process $Rh^{II}_2 \rightleftharpoons Rh^{II}Rh^{III}$ is immediately followed by a chemical reaction which is most likely a ligand-substitution reaction at the axial site or demethylation of the axial ether group. Numerous efforts to obtain single crystals of this product failed to give other than a powder form.

X-ray Structure of 1. The title compound was recrystallized from EtOH and Et_2O to give green crystals, one of which was examined by single-crystal X-ray diffraction methods. The important bond distances and angles for **1** are given in Table III. All other information pertaining to the refinement can be found in the supplementary material. An ORTEP plot of the molecular structure with the atom-labeling scheme is shown in Figure 6. The molecule contains an unusually bonded η^3, μ-TMPP ligand as previously described.[6h] Of particular note in this structure is the transformation of an ether group on the phosphine to a phenoxide, thus allowing for a stable Rh(1)–P(1)–C(7)–C(8)–O(7)–Rh(2) metallacycle to form. The Rh(2)–O(7) bond distance of 2.048 (2) Å is substantially shorter than the axial ether interaction Rh(1)–O(10) of 2.351 (2) Å. Other metric parameters within the molecule are within usual ranges for dirhodium(II,II) complexes.[11] The Rh–Rh bond distance of 2.4228 (3) Å is slightly longer than that found for the complex $Rh_2(O_2CCH_3)_4(MeOH)_2$ in which r(Rh–Rh) = 2.377 Å.[11]

Conclusion

The presence of hard and soft donor atoms of varying degrees of nucleophilicity in a binuclear metal complex is an interesting combination. The unsymmetrical complex $Rh_2(\mu\text{-}O_2CCH_3)_3(\eta^3\text{-}\mu\text{-TMPP-}O)$ possesses a unique phosphino phenoxide bridging group and a tethered axial ether moiety in addition to three bridging acetate groups. This molecule represents a rare opportunity to study the effects of a mixed-ligand environment (i.e. carboxylate, phenoxide, phosphine, and ether groups) on the chemistry of an important dimetal unit. Future work on this system will focus on selective removal of the carboxylate ligands to open up sites of reactivity.

Acknowledgment. We thank Dr. Long Le for help with the NMR experiments and Steven Haefner for the EPR data. We are grateful to the National Science Foundation for instrumentation grants (X-ray, CHE-8403823, and NMR, CHE-8800770) and a grant to the PI (CHE-8914915). Mass spectral data were obtained at the Michigan State University Mass Spectrometry Facility, which is supported, in part, by a grant (DRR-00480) from the Biotechnology Resources Branch, Division of Research Resources, National Institutes of Health. Grateful acknowledgement is also made to Johnson Matthey for a loan of $RhCl_3 \cdot xH_2O$.

Supplementary Material Available: Tables of crystallographic parameters, full bond distances and angles, and anisotropic thermal parameters (10 pages); a listing of structure factors (35 pages). Ordering information is given on any current masthead page.

(11) (a) Felthouse, T. R. *Prog. Inorg. Chem.* **1982**, *29*, 73. (b) Boyar, E. B.; Robinson, S. D. *Coord. Chem. Rev.* **1983**, *50*, 109.